Structural changes in the recombinant, NADP(H)-binding component of proton translocating transhydrogenase revealed by NMR spectroscopy

Philip G. Quirk, Mark Jeeves, Nick P.J. Cotton, John K. Smith, Baz J. Jackson*

School of Biochemistry, University of Birmingham, Edgbaston, Birmingham B15 2TT, UK

Received 13 December 1998; received in revised form 25 January 1999

Abstract We have analysed ^{1}H, ^{15}N-HSQC spectra of the recombinant, NADP(H)-binding component of transhydrogenase in the context of the emerging three dimensional structure of the protein. Chemical shift perturbations of amino acid residues following replacement of $NADP^+$ with NADPH were observed in both the adenosine and nicotinamide parts of the dinucleotide binding site and in a region which straddles the protein. These observations reflect the structural changes resulting from hydride transfer. The interactions between the recombinant, NADP(H)-binding component and its partner, NAD(H)-binding protein, are complicated. Helix B of the recombinant, NADP(H)-binding component may play an important role in the binding process.

Key words: Transhydrogenase; NMR; Nicotinamide nucleotide; Model structure; *Rhodospirillum rubrum*

1. Introduction

Transhydrogenase, found in bacteria and animal mitochondria, couples the transfer of reducing equivalents between NAD(H) and NADP(H) to the translocation of protons across a membrane. For recent reviews, see [1–3]. The reaction is driven from left to right, in the following equation, by the energy of the proton electrochemical gradient (Δp), generated by respiratory or photosynthetic electron transport.

$$NADH + NADP^+ + nH^+_{OUT} \Leftrightarrow NAD^+ + NADPH + nH^+_{IN} \quad (1)$$

Where n is probably 1 [4]. The protein has a tripartite structure. The NAD(H)-binding protein (dI) component, which binds NAD^+ and NADH and the recombinant, NADP(H)-binding (dIII) component, which binds $NADP^+$ and NADPH, protrude from the membrane, while dII spans the membrane. Recombinant forms of dI and dIII have been isolated from transhydrogenases of several species [5–10]. Remarkably, a mixture of the two proteins, even in the absence of dII, gives a complex which can catalyse transhydrogenation [7–12].

The dIII component is particularly interesting because it binds $NADP^+$ and NADPH very tightly in the absence of dII [8]. On the dIII protein, NADPH is stabilised relative to $NADP^+$, thus increasing the nucleotide redox potential [13]. We have proposed that, in the complete enzyme, the coupling between transhydrogenation and Δp is achieved through alterations in the binding energies of the protein for $NADP^+$ and NADPH [1,8,13,14]. Interestingly, the binding of $NADP^+$ and NADPH, either to the complete enzyme or to isolated dIII, leads to protein conformational changes that can be detected by Trp fluorescence, circular dichroism [9] or changes in susceptibility to proteolysis [15], though it remains to be established which, if any, of these conformational changes are of significance in the process of energy coupling.

In this report we use NMR spectroscopy to identify two classes of amino acid residues in the recombinant dIII protein from *Rhodospirillum rubrum* transhydrogenase: (a) those whose micro environment is altered by replacement of $NADP^+$ with NADPH and (b) those affected by the binding of dI protein. These observations will help to define which amino acid residues are involved in conformational changes that occur at the NADP(H)-binding site during the transhydrogenation reaction and which residues on dIII might be involved in an interaction with dI. The residues are mapped on to our emerging NMR structure of the dIII protein [16]. The existence of a GXGXXA/V sequence motif in dIII led to the suggestion [17–19] that dIII might have a typical dinucleotide-binding fold [20]. On this basis, Fjellström et al. [21] devised a partial model of the *Escherichia coli* dIII protein using the secondary structure predictions of the PHD programm [22]. Below, we use a different algorithm to generate a model of *R. rubrum* dIII. ^{1}H-^{1}H NOE data, interpreted using our recently published NMR assignments [16], provide support for the model but also reveal interesting differences from the archetypal dinucleotide-binding fold.

Some of the results reported below, including the preliminary NMR structure, were described on a poster presented at the 10th European Bioenergetics Meeting, Gothenburg, June 1998.

2. Materials and methods

The dI and dIII proteins of *R. rubrum* transhydrogenase were expressed in *E. coli* from the plasmids pCD1 [5] and pNIC2 [16], respectively. The dI protein was isolated and purified as described [5]. Isotopically labelled dIII protein was extracted from cells grown in M9 medium [23], in which $[^{15}N]NH_4Cl$ was the sole nitrogen source and purified by column chromatography, in buffer containing 4 μM $NADP^+$ [8]. The dIII protein, as isolated, contains approximately one mole of tightly bound nucleotide, a mixture of $NADP^+$ and NADPH, per mole of protein. We have been unable to remove this bound nucleotide without the protein precipitating, but we can convert it into fully oxidised or fully reduced forms. Residual NADPH on the dIII protein was oxidised with dI plus $AcPdAD^+$, followed by further chromatography [16]. Replacement of $NADP^+$ on dIII with NADPH was achieved through incubation with 100 μM reduced nucleotide for 4 h (protein concentration ~30 μM). Excess NADPH was then removed by filtration (Vivascience, 5 kDa cut-off) [24]. The purity of the proteins was routinely examined by SDS-PAGE and protein concentrations were estimated by the microtannin procedure [25], values given in the figure legends refer to the concentration of monomers.

*Corresponding author. Fax: (44) (0) 121 414 3982.
E-mail: j.b.jackson@bham.ac.uk

PII: S0014-5793(99)00198-2

```
  1  MNRSIFNVIL GGFGSEGGVA AAGGAAGDRS VKAGSAEDAA FIMKNASKVI
            SSS SS       SS SS    HHHHH HHHHHHHHHH HHHHTTTTSS
                                     BBBBBHHHHH HHHH  BBBB
                                               □□   □□□ □

 51  IVPGYGMAVA QAQHALREMA DVLKKEGVEV SYAIHPVAGR MPGHMNVLLA
     SSTTT  HHH HHHHHHHHHH HHHHHH     SSSSSSSS    TT HHHHHH
     B   HHHHH    HHHHHHHH HHHHH    B BBBBBBB       HHHHHHH
     □  □     □   □  □□□□□ □□□□   □□  □□□□□ □           □□□

101  EANVPYDEVF ELEEINSSFQ TADVAFVIGA NDVTNPAAKT DPSSPIYGMP
     HHHHHHHHHH HHHHHH       SSSSSS T T
     H               HHHHH    BBBBB          BB B  B
        □                     □□□□□□□   □□

151  ILDVEKAGTV LFIKRSMASG YAGVENELFF RNNTMMLFGD AKKMTEQIVQ
              S SSS   HHHH HHHHHHHHH  TTT  SSSS  HHHHHHHHHH
            BB BBBB                    BBBBBB   HHHHHHHHHH
        □□ □□□□ □ □□                □□□ □  □□□□□□     □□□□□□

201  AMN

     HH
     □
```

Fig. 1. Amino acid sequence of the recombinant dIII protein of *R. rubrum* transhydrogenase, conserved residues, secondary structure predictions and $^{1}H/^{2}H$ exchange. The top row shows the amino acid sequence of the recombinant dIII protein of *R. rubrum* transhydrogenase. Residues which are invariant in 10 other available sequences are printed in bold type. The second row shows secondary structure predictions of the PSA programme [27]: H = helix, B = β strand, T = turn. The third row shows the predictions of secondary structure, based on chemical shift indexing [28]. The fourth row shows $^{1}H/^{2}H$ exchange with the □ symbol indicating amide protons which had only partially exchanged with solvent deuterons over a 5 h period.

The dI and dIII proteins were prepared for NMR spectroscopy as described [6,16].

All NMR experiments reported here were performed on a Bruker AMX 500 spectrometer, operating at 500.13 MHz for ^{1}H. The ^{1}H, ^{15}N-HSQC experiments were performed using the FHSQC pulse sequence [26] with a relaxation delay of 1 s between each scan. The spectral widths were 7575 Hz in the ^{1}H dimension and 1723 Hz in the ^{15}N dimension. 1 K data points were collected in the direct dimension and 256 rows in the indirect dimension, each comprising between 16 and 64 scans. Experiments were performed at 30°C and pH 7.2, unless otherwise stated.

For the titration of dI into dIII, aliquots of unlabelled dI protein were added in separate experiments to $NADP^{+}$- or NADPH-bound dIII and ^{1}H, ^{15}N-HSQC spectra were acquired over a range of dI:dIII concentration ratios between 1:75 and 1:1. In these experiments, both dI and dIII were prepared in buffer containing 8% $^{2}H_2O$, 10 mM HEPES, pH 7.2, 10 mM $(NH_4)_2SO_4$, 0.15% sodium azide, 10 μM $NADP^{+}$ or NADPH and 1 mM DTT.

For the investigation of amide proton exchange rates, dIII was prepared in $^{1}H_2O$ buffer. The $^{1}H_2O$ was exchanged for $^{2}H_2O$ by repeated washing of the protein solution with deuterated buffer, followed by filter concentration (Vivascience, 5 kDa cut-off). This was performed at 4°C and took approximately 3 h. The sample was transferred to the NMR tube and incubated at 30°C for a further 2 h before acquisition of the HSQC spectrum.

3. Results

Fig. 1 shows the amino acid sequence of our recombinant dIII protein of *R. rubrum* transhydrogenase. The N-terminal

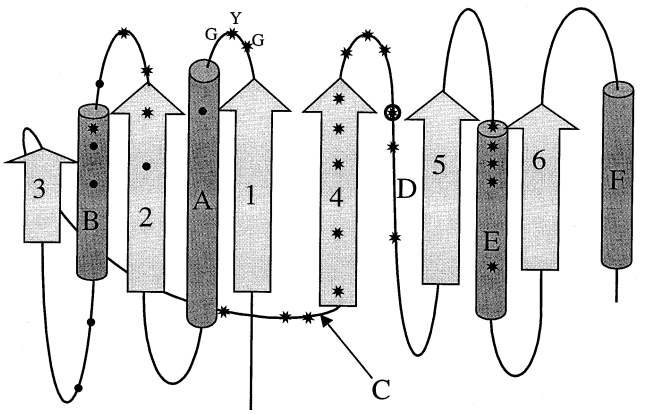

Fig. 2. Model of the secondary structure of the recombinant dIII protein of *R. rubrum* transhydrogenase. The model is based on the secondary structure predictions shown in Fig. 1 and on NOEs identified from ^{15}N- and ^{13}C-resolved NOESY experiments (M. Jeeves et al., unpublished observations). We have adopted the system of Branden and Tooze [31] for naming the strands and helices. The limits of the strands and helices (from NOEs) are as follows: β1, residues 46–52; β2, 79–85; β3, 124–128; β4, 137–144; β5, 160–166; β6, 184–189; αA, 55–76; αB, 94–102; αE, 171–180; αF, 191–200. * Amino acid residues whose resonances in the ^{1}H, ^{15}N-HSQC spectrum are shifted upon substitution of $NADP^{+}$ by NADPH (see Table 1). ● Amino acid residues whose resonances in the ^{1}H, ^{15}N-HSQC spectrum are characterised by intermediate exchange with dI protein (see Fig. 3). ○ Gly-148, see text.

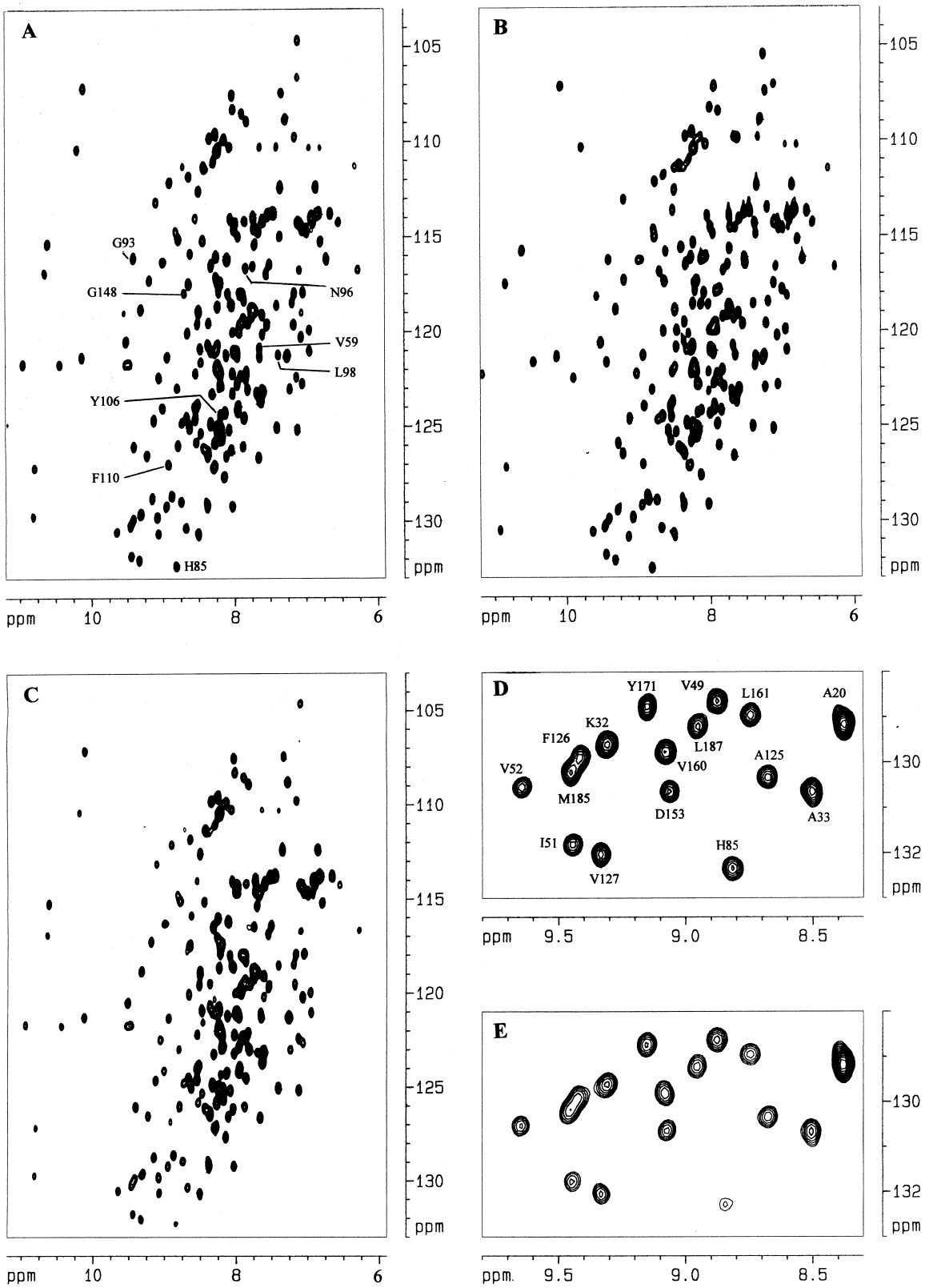

Fig. 3. ^{1}H, ^{15}N-HSQC spectra of the recombinant dIII protein of *R. rubrum* transhydrogenase. (A) Spectrum of 600 μM dIII protein complexed with $NADP^{+}$ (complete assignments are given elsewhere [16]). Assignments of the eight residues whose intensities are considerably decreased upon addition of dI protein (class (3), see text) are given. (B) Spectrum of 500 μM dIII protein complexed with NADPH. (C) Spectrum of 500 μM dIII.$NADP^{+}$ in the presence of 70 μM dI protein. (D) and (E) Expanded portions of (A) and (C), respectively, to illustrate the three classes of resonance behaviour described in the text: class (1) Ala-20, class (3) His-85, class (2) the rest. The peak height of the Ala-20 resonance was used as an internal reference and the spectra were scaled accordingly.

Table 1
Chemical shift mapping of dIII protein upon replacement of $NADP^+$ by NADPH

Residue	$NADP^+$ bound		NADPH bound		Chemical shift perturbation (Hz)
	HN	N	Δ HN	Δ N	
Gly-54	7.35	107.16	−0.10	0.13	55.9
Tyr-55	9.52	121.57	0.39	0.79	234.9
Ala-88	8.12	126.48	†	†	†
Gly-89	10.21	110.16	−0.41	0.06	206.3
Met-91	7.61	120.02	0.07	−0.82	75.2
Met-95	9.11	112.96	0.11	−0.01	54.5
Asn-131	10.66	116.73	0.20	0.65	133.9
Asp-132	10.81	129.64	0.12	0.74	99.3
Val-133	7.11	104.37	0.16	0.94	125.9
Asn-135	7.13	122.27	0.26	−0.58	160.8
Ala-137	8.79	125.90	†	†	†
Lys-139	7.85	113.97	†	†	†
Thr-140	7.83	108.69	−0.20	1.04	150.4
Asp-141	8.32	123.16	†	†	†
Ser-143	7.99	114.07	0.25	1.13	183.5
Ser-144	8.11	121.10	†	†	†
Ile-146	7.16	109.53	0.18	0.16	99.1
Gly-148	8.70	117.82	0.02	−1.08	63.2
Met-149	8.04	126.13	−0.13	−1.35	132.4
Val-154	7.56	116.73	−0.02	−0.78	50.5
Gly-170	8.91	111.93	−0.12	0.11	66.7
Tyr-171	9.16	128.69	−0.28	−0.01	142.0
Ala-172	10.97	121.60	0.21	0.52	130.4
Gly-173	8.04	107.29	−0.08	−0.29	55.3
Glu-177	9.42	125.93	−0.12	−0.18	54.5

The first two columns indicate the amide ^1H and ^{15}N chemical shifts (ppm) for the $NADP^+$-bound protein. Columns 3 and 4 indicate the chemical shift changes (in ppm, where 1 ppm ≡ 500.13 Hz) following substitution by NADPH. A negative value indicates an upfield movement. The chemical shift perturbation (column 5) for each residue was calculated as described in the text: the table lists the residues for which this value exceeded 50 Hz. Residues indicated by † have not yet been definitively assigned in NADPH-bound dIII but show large chemical shift perturbations (> 50 Hz).

residue (Met-1) corresponds to Met-262 of the β subunit of the complete enzyme [8]. Residues that are invariant in the 10 other, currently available, transhydrogenase sequences are printed in bold type. The second row in the figure gives the predictions of secondary structure elements using the PSA program of Stultz, White and Smith [27], accessed through the PSA web site (http://bmerc-www.bu.edu/psa). The algorithm is based on comparisons between overlapping segments of the sequence and known three dimensional structures. The third row in Fig. 1 gives predictions of α helix and β strand in dIII, based on chemical shift indexing of the H^α, C^α, C^β and C' atoms in the protein backbone [28], using software available at the web site http://www.pence.ualberta.ca. In this method, the chemical shifts of several signals from each residue are scored and placed within one of three classes: random coil, helical or sheet (the boundaries of these classes having been determined empirically). The location of helices and sheets is indicated by the occurrence of continuous groups of signals lying within the corresponding class. There is reasonable, though not perfect, agreement between the two sets of predictions. The fourth row in Fig. 1 shows the extent to which ^1H atoms bound to the backbone amide nitrogen atoms of the dIII protein exchange with solvent ^2H_2O during a period of approximately 5 h. Generally, hydrogen/deuterium exchange is slow in segments of proteins with extensive hydrogen bonding, for example in α helices and, particularly, in β sheet. The data with the dIII protein show that all the predicted β strand residues, apart from those of strand 4 (and, to some extent, those in strand 1), and about half the predicted α helix residues, are indeed slow to exchange, whereas the turns between these elements of secondary structure exhibit a rapid exchange. No amide proton signals remained after 24 h incubation in ^2H_2O buffer at 30°C.

Fig. 2 shows a structural model partly based on the predictions of Fig. 1, but modified on the basis of ^1H-^1H NOEs observed in a series of ^{15}N- and ^{13}C-resolved NOESY experiments (M. Jeeves et al., unpublished data). Importantly, the NOEs establish (a) the locations of the β strands and α helices in the polypeptide chain (see figure legend) and (b) the relative positions of adjacent strands and the fact that they are aligned in a parallel β sheet. NOEs between strands β1 and β4 reveal a line of symmetry between two β-α-β motifs. The model and NOE information show that the dIII protein has the structure of a Rossmann dinucleotide-binding fold [20]. However, there are clear indications that some features of dIII are atypical. 'Helix D', found in other Rossmann structures, is not predicted by the modelling program and, to date, we have not found NOEs that are consistent with the helical character in this segment of the polypeptide chain. Interestingly, the secondary structure predictions also failed to reveal β4, but this strand is predicted by the chemical shift indexing and by NOEs to β1. As will be evident from the effects of nucleotide replacement (see below), this promises to be an interesting region of the protein. Note that both the modelling, the chemical shift indexing and a lack of NOEs suggest that N-terminal residues 1–25 are disordered. However, there is some secondary structure in the segment of polypeptide from residues 26–45 before the first strand of the Rossmann fold. NADP(H) is expected to bind in a shallow crevice outside the C-terminal ends of strands β1 and β4 with the adenosine moiety located in the first β-α-β mononucleotide-binding region (β1-αA-β2-αB-β3), the nicotinamide-ribose moiety located in the second

(β4-loop D-β5-αE-β6) and with the pyrophosphate group adjacent to the glycine-rich turn between strand β1 and helix αA.

Fig. 3A shows the ^{1}H, ^{15}N-HSQC spectrum of ^{15}N-labelled dIII protein in its $NADP^+$-bound form. In this spectrum, each amide H atom is correlated to its chemically bonded N atom. Almost all the peaks have been assigned from triple resonance experiments [16]. Those remaining unassigned originate either from side chain amides or from the 12 N-terminal residues. In addition, 171 residues have been assigned in the HSQC spectrum of dIII.NADPH, by comparison with that of dIII.$NADP^+$. When the bound $NADP^+$ was exchanged for NADPH (see Section 2), about 40 of the total ~230 peaks were shifted in the ^{1}H and/or ^{15}N dimensions (Fig. 3B), indicating a change in the magnetic environment of the -NH group. Such perturbations could arise either from changes in the local protein conformation or from altered interactions with the nucleotide cofactor. In order to quantify the changes, the chemical shift perturbation was defined as the sum of the absolute values of the individual ^{1}H and ^{15}N movements, expressed in Hz [29]. For the 171 assigned residues, the mean perturbation was 25 Hz and we have chosen a threshold value of 50 Hz as indicating a substantial change in environment. The amino acid residues whose chemical shift perturbations exceeded 50 Hz are listed in Table 1 and their positions are mapped onto the structural model, using the * symbol (Fig. 2). The protein seems not to be globally affected by nucleotide replacement, instead, the changes appear to be clustered into two areas. (1) There are shifts of resonances attributable to amino acid residues that are located in the vicinity of the bound nucleotide (see above). Unexpectedly, the backbone -NH groups of amino acid residues close to the binding pocket of both the adenosine moiety and the nicotinamide mononucleotide moiety are influenced by the substitution, as well as those in the glycine-rich pyrophosphate-binding region. (2) Replacement of bound $NADP^+$ with NADPH results in a 'spur' of magnetic change which descends the full lengths of strand β4 (and into the C-terminus of the 'crossover' loop C), 'loop D' (see above) and helix E.

Fig. 3C shows the effect on the HSQC spectrum of the $NADP^+$-loaded dIII protein (500 μM) of adding isotopically unlabelled dI protein from *R. rubrum* transhydrogenase (70 μM). Three classes of behaviour were observed, as illustrated by the expanded section of the spectrum shown in Fig. 3D,E. (1) The peaks assigned to the N-terminus (residues 1–31) and C-terminus (residue 203) of the protein were unaffected by the addition of dI protein. (2) For the majority of the peaks in the HSQC spectrum, addition of dI protein led to partial loss of signal intensity (25–40%). (3) The signals from eight backbone (V59, H85, G93, N96, L98, Y106, F110, G148) and four side chain (not yet assigned) amides suffered a more pronounced loss of intensity (>75%). On the structural model, five of the amino acid residues assigned to this group of resonances clustered in and around helix B and there were single representatives in the adjacent helix A and strand 2 (see the ● symbols in Fig. 2). Interestingly, the signal from G148, located in loop D and labelled ○ in Fig. 2, also underwent an upfield shift in both the ^{1}H (>0.01 ppm) and ^{15}N (>0.2 ppm) dimensions, moving partially under that of E37. None of the other residues was shifted significantly. At higher concentrations of dI protein (200 μM, dI:dIII ratio of 1:1), dIII resonances in the first class again showed little change in intensity and resonances in the second and third classes continued the trends observed at low dI concentration (data not shown).

The experiment shown in Fig. 3C was also performed with dIII protein loaded with NADPH instead of $NADP^+$. Upon addition of dI protein, the same three classes of behaviour of resonances in the HSQC spectrum were observed (data not shown). There were some slight differences in the behaviour of the class (3) resonances: notably H85, Y106 and F110 were less affected than with dIII.$NADP^+$ but V59, G93, N96 and the sensitive side chain amide NH groups were affected in the same way. The addition of dI to dIII.NADPH did not lead to a detectable change in the chemical shift of G148 but did cause broadening comparable to that of the other class (3) resonances.

Four of the class (3) resonances (V59, G93, N96, L98) exhibited much less broadening when the HSQC experiment in the presence of dI protein was performed at 20°C instead of 30°C. This is a clear indication that these residues were in intermediate exchange on the NMR time scale at the higher temperature, moving to the slow exchange region upon cooling. Similarly, many class (2) resonances gained some intensity at the lower temperature, as their initially slow intermediate exchange rates decreased further towards the slow limit.

4. Discussion

Chemical shift perturbations revealed by ^{1}H, ^{15}N-HSQC experiments indicate alterations in the magnetic environment of nuclei, but cannot be rigorously interpreted in terms of specific changes in the protein structure. Nevertheless, the locations of residues of dIII undergoing large perturbations, following substitution of NADPH for $NADP^+$, provide a strong indication of regions of the protein where structural changes might be taking place. A lack of chemical shift change for part of the backbone, however, cannot necessarily be interpreted as indicating an absence of conformational change in that region.

Differences between the solution structures of $NADP^+$ and NADPH are mainly confined to the nicotinamide rings. In the oxidised nucleotide, the ring is aromatic, cationic and almost planar, whereas the dihydronicotinamide ring is uncharged and puckered [30]. However, the HSQC spectra indicate possible structural changes in both the adenosine- and the nicotinamide-binding parts of the dIII protein when NADPH is substituted for $NADP^+$ (Fig. 3A,B). Thus, during catalytic turnover, a conformational change, propagated by reduction of the nicotinamide ring, is transmitted to the adenosine-binding region. Transmission could occur either directly, through the rigidity of the bound dinucleotide, or indirectly, through changes in orientation of the protein strands and helices. A second set of chemical shift changes, resulting from replacement of $NADP^+$ by NADPH, occurs along strand β4 (into loop C), loop D and helix E. Interestingly, this change in the magnetic environment seems to straddle the protein in a region which shows some deviation from the archetypal Rossmann structure. In our working model for the mechanism of transhydrogenase [1,8,13,14], the binding of substrate $NADP^+$ and the release of product NADPH take place in an 'open state' of dIII, whereas transfer of the hydride ion from NADH to $NADP^+$ occurs within an 'occluded state' in which NADPH is stabilised relative to $NADP^+$ and in which both these nucleotides are very slow to exchange with the solvent.

Appropriately gated power strokes use the energy of Δp to drive the enzyme firstly from the open state to the occluded state and then, following hydride transfer, from the occluded state to the open state. Isolated dIII is locked into the occluded state [8]. We therefore envisage that the changes in the HSQC spectrum, described above, reflect changes in the conformation that are required, following conversion of $NADP^+$ to NADPH (by hydride transfer from NADH), to prime dIII ready for the second power stroke and/or the associated gating processes.

Analysis of steady state [8] and stopped flow [24] experiments indicates that the K_d for the dissociation of the catalytic dI:dIII complex is $< 10^{-6}$ M and that the k_{off} value is approximately 50/s. In the conditions of the experiment shown in Fig. 3C and E, it follows that the exchange rate between dIII, in its free and its complexed forms, will be relatively slow on the NMR time scale. Due to a longer correlation time, the T_2 of the catalytic complex will be significantly shorter than that of isolated dIII and therefore the apparent loss of intensity in the majority of the peaks upon addition of dI (class (2), Fig. 3C and E) can be explained on the basis of signal broadening resulting from this slow-intermediate exchange. Those peaks in the HSQC spectrum which remain unaffected by addition of dI (class (1)) are located predominantly at the N-terminus of dIII, suggesting that this region of the protein retains a high degree of segmental mobility despite formation of the complex. This is consistent with the finding that the N-terminal region of recombinant dIII seems to be rather unstructured. Those 12 peaks in the HSQC spectrum which undergo an apparent intensity loss due to intermediate exchange upon addition of dI (class (3)) reflect a lower affinity binding process (K_d of the order of 10^{-5} M). This phenomenon might arise from the fact that the dI protein is dimeric [5] while the dIII protein is monomeric. It is unlikely to represent an initial recognition of the dI dimer by the first dIII molecule, since such a complex would be converted rapidly into the tight, slowly exchanging $(dI)_2$.(dIII) complex, responsible for the behaviour of the class (2) amides. Instead, we suggest that this lower affinity process corresponds to the addition of a second molecule of dIII to the $(dI)_2$.(dIII) complex, i.e. $dIII+(dI)_2.dIII \Leftrightarrow (dI)_2.(dIII)_2$. This interpretation is consistent with stopped flow experiments on the formation of the catalytic complex, which were interpreted as evidence that the second dIII binds to the dI dimer with a K_d of 20–50 μM [24]. Assuming that the second dIII binds at its proper site, this indicates that the region in and around helix B is mainly responsible for the initial interaction with dI.

Acknowledgements: We are grateful to the Biotechnology and Biological Sciences Research Council and the Wellcome Trust for financial support and we thank Jamie Venning for the discussion. We also thank Dr. Jan Rydström and colleagues for sending us a copy of their model of the *E. coli* dIII protein, based on the secondary structure predictions of the PHD program [22].

References

[1] Jackson, J.B., Quirk, P.G., Cotton, N.P.J., Venning, J.D., Gupta, S., Bizouarn, T., Peake, S.J. and Thomas, C.M. (1998) Biochim. Biophys. Acta 1365, 79–86.
[2] Rydström, J., Hu, X., Fjellström, O., Meuller, J., Zhang, J., Johansson, K. and Bizouarn, T. (1998) Biochim. Biophys. Acta 1365, 10–16.
[3] Bragg, P.D. (1998) Biochim. Biophys. Acta 1365, 98–104.
[4] Bizouarn, T., Sazanov, L.A., Aubourg, S. and Jackson, J.B. (1996) Biochim. Biophys. Acta 1273, 4–12.
[5] Diggle, C., Hutton, M., Jones, G.R., Thomas, C.M. and Jackson, J.B. (1995) Eur. J. Biochem. 228, 719–726.
[6] Diggle, C., Cotton, N.P.J., Grimley, R.L., Quirk, P.G., Thomas, C.M. and Jackson, J.B. (1995) Eur. J. Biochem. 232, 315–326.
[7] Yamaguchi, M. and Hatefi, Y. (1995) J. Biol. Chem. 270, 28165–28168.
[8] Diggle, C., Bizouarn, T., Cotton, N.P.J. and Jackson, J.B. (1996) Eur. J. Biochem. 241, 162–170.
[9] Fjellström, O., Johansson, C. and Rydström, J. (1997) Biochemistry 36, 11331–11341.
[10] Peake, S.J., Venning, J.D. and Jackson, J.B. (1998) Biochim. Biophys. Acta, (in press).
[11] Yamaguchi, M. and Hatefi, Y. (1997) Biochim. Biophys. Acta 1318, 225–234.
[12] Fjellström, O., Bizouarn, T., Zhang, J., Rydström, J., Venning, J.D. and Jackson, J.B. (1998) Biochemistry, (in press).
[13] Venning, J.D. and Jackson, J.B. (1999) (submitted).
[14] Hutton, M.N., Day, J.M. and Jackson, J.B. (1994) Eur. J. Biochem. 219, 1041–1051.
[15] Tong, R.C.W., Glavas, N.A. and Bragg, P.D. (1991) Biochim. Biophys. Acta 1080, 19–28.
[16] Jeeves, M., Smith, K.J., Quirk, P.G., Cotton, N.P.J. and Jackson, J.B. (1999) J. Biomol. NMR, (in press).
[17] Hu, P.S., Persson, B., Hoog, J.O., Jornvall, H., Hartog, A.F., Berden, J.A., Holmberg, E. and Rydström, J. (1992) Biochim. Biophys. Acta 1102, 19–29.
[18] Glavas, N.A. and Bragg, P.D. (1995) Biochem. Mol. Biol. Int. 35, 297–306.
[19] Olausson, T., Fjellström, O., Meuller, J. and Rydström, J. (1995) Biochim. Biophys. Acta 1231, 1–19.
[20] Eventoff, W. and Rossmann, M.G. (1975) CRC Crit. Rev. Biochem. 111, 111–140.
[21] Fjellström, O., Axelsson, M., Bizouarn, T., Hu, X., Johansson, C. and Rydström, J. (1998) personal communication.
[22] Rost, B. and Sander, C. (1994) Proteins 20, 216–226.
[23] Sambrook, J., Fritsch, E.F. and Maniatis, T. (1989) Molecular Cloning, A Laboratory Manual, Cold Spring Harbor Laboratory Press.
[24] Venning, J.D., Bizouarn, T., Cotton, N.P.J., Quirk, P.G. and Jackson, J.B. (1998) Eur. J. Biochem. 257, 202–209.
[25] Mejbaum-Katzenellenbogen, S. and Drobryszycka, W.J. (1959) Clin. Chem. Acta 4, 515–522.
[26] Mori, S., Abeyguanawardana, C., Johnson, M.O. and Vanzyl, P. (1995) J. Magn. Reson. Ser. B 108, 94–98.
[27] Stultz, C.M., White, J.V. and Smith, T.F. (1993) Protein Sci. 2, 305–314.
[28] Wishart, D.S. and Sykes, B.D. (1994) Meth. Enzymol. 239, 363–392.
[29] Lee, A.L., Volkman, B.F., Robertson, S.A., Rudner, D.Z., Barbash, D.A., Cline, T.W., Kanaar, R., Rio, D.C. and Wemmer, D.E. (1997) Biochemistry 36, 14306–14317.
[30] Grau, U.M. (1982) in: The Pyridine Nucleotide Coenzymes (Everse, J., Andersom, B. and You, K.S., Eds.), pp. 135–187, Academic Press, New York.
[31] Branden, C. and Tooze, J. (1991) Introduction to Protein Structure, Garland, New York.